Effects of Solution Conditions on Virus Retention by the Viresolve® NFP Filter

Shudipto K. Dishari, Matthew R. Micklin, Ki-Joo Sung, and Andrew L. Zydney
Dept. of Chemical Engineering, The Pennsylvania State University, University Park, PA 16802

Adith Venkiteshwaran and Jennifer N. Earley
Dept. of Bioproduct Research, Eli Lilly and Company, Indianapolis, IN 46285

DOI 10.1002/btpr.2125
Published online June 25, 2015 in Wiley Online Library (wileyonlinelibrary.com)

Virus filtration can provide a robust method for removal of adventitious parvoviruses in the production of biotherapeutics. Although virus filtration is typically thought to function by a purely size-based removal mechanism, there is limited data in the literature indicating that virus retention is a function of solution conditions. The objective of this work was to examine the effect of solution pH and ionic strength on virus retention by the Viresolve® NFP membrane. Data were obtained using the bacteriophage ϕX174 as a model virus, with retention data complemented by the use of confocal microscopy to directly visualize capture of fluorescently labeled ϕX174 within the filter. Virus retention was greatest at low pH and low ionic strength, conditions under which there was an attractive electrostatic interaction between the negatively charged membrane and the positively charged phage. In addition, the transient increase in virus transmission seen in response to a pressure disruption at pH 7.8 and 10 was completely absent at pH 4.9, suggesting that the trapped virus are unable to overcome the electrostatic attraction and diffuse out of the pores when the pressure is released. Further confirmation of this physical picture was provided by confocal microscopy. Images obtained at pH 10 showed the migration of previously captured phage; this phenomenon was absent at pH 4.9. These results provide important new insights into the factors governing virus retention using virus filtration membranes. © 2015 American Institute of Chemical Engineers *Biotechnol. Prog.*, 31:1280–1286, 2015
Keywords: virus filtration, pressure disruption, retention, electrostatic interactions, bioprocessing

Introduction

Viral clearance is an essential part of the downstream process in the production of nearly all biopharmaceuticals. Viral contamination can occur through engineered cell lines, contaminated raw materials or media, and the manufacturing environment. Multiple processing steps are used to ensure inactivation and/or removal of all viruses, with the specifics depending upon the nature of the biological product and the risks inherent in the manufacturing process.[1] Current efforts typically employ a virus filtration step using membranes with ~20 nm pore size. These virus filters provide a robust method for virus removal that complements virus inactivation (e.g., low pH hold) and adsorptive processes (e.g., ion exchange and affinity chromatography) used in the production of monoclonal antibody products.[1,22]

Although virus filtration is typically thought to provide a purely size-based viral clearance,[21] several studies have shown that virus retention is a function of solution pH,[2] salt concentration,[3,4] and even the type of ions.[5,6] These effects are commonly attributed to differences in the contribution of virus sorption,[6] the level of virus aggregation,[7] and/or the formation of protein-virus complexes.[8] For example, Hirasaki et al.[9] observed a loss in virus retention by the Planova filter in the presence of Tween 80, which the authors attributed to a reduction in available sites for virus capture. Lukasik et al.[6] found a similar reduction in virus retention with several other filters upon addition of Tween or urea, which they attributed to a reduction in hydrophobic interactions between the virus and the membrane surface. Oshima et al.[3] obtained significant removal of pp7 (a model bacteriophage) by the Pall DV50 membrane when using ultrapure water, but this largely disappeared when the phage were suspended in Dulbecco's phosphate buffered saline (PBS). In contrast, Yokoyama et al.[5] found very high removal of human parvovirus B19 when using 0.3 M glycine but minimal removal when the virus was suspended in water or PBS. The reason for the very different dependence on buffer is unclear. Virus removal was also a function of solution pH, with maximum removal when the virus was essentially uncharged (i.e., near the isoelectric point of the virus at pH 6). There is also strong evidence for the role of electrostatic interactions on virus clearance using depth filtration.[23]

Woods and Zydney[10] and Dishari et al.[11] have shown that confocal microscopy can provide important insights into the key phenomena governing virus capture during virus

Current address of Ki-Joo Sung: University of Michigan
Current address of Adith Venkiteshwaran: Harvard Business School
Correspondence concerning this article should be addressed to: A. Zydney at zydney@engr.psu.edu.

filtration. This includes both the decline in virus retention seen in some virus filtration experiments[12] as well as the transient jump in virus transmission seen in response to a disruption in the filtration process.[10] In particular, Dishari et al.[11] developed a novel two-dye approach to visualize the capture of viruses before and after a disruption in the filtration pressure.

The objective of this study was to examine the effect of solution pH and ionic strength on virus capture using the Viresolve® NFP parvovirus filter, a highly asymmetric commercially available virus filter sold by EMD Millipore. Data were obtained with the bacteriophage ϕX174 using plaque forming assays to evaluate the degree of virus retention during both constant pressure experiments and in filtration runs with a pressure disruption. For pressure disruption experiments, confocal images were obtained using phage labeled with different fluorescent dyes to separately visualize the phage that were in the challenge solution before and after the pressure disruption. These results provide important insights into the physical phenomena controlling virus retention in the Viresolve® NFP parvovirus filter.

Materials and Methods

Membranes

Viresolve® NFP membranes were provided by EMD Millipore (Bedford, MA) in a flat sheet (single layer) format. Small circular disks were cut from the sheet using a specially designed cutting device in our laboratory.

Bacteriophage

Experiments were performed with bacteriophage ϕX174 (ATCC-13706-B1™), obtained from the American Type Culture Collection (ATCC, Manassas, VA), as a model parvovirus. Luria-Bertani (LB) media was prepared by mixing 10 g L^{-1} Bacto™ Tryptone (BD-211705), 5 g L^{-1} Bacto Yeast extract (BD-212750), and 10 g L^{-1} NaCl in deionized water. The pH was adjusted to 7.5 using NaOH, and the media was then autoclaved and stored in a sterilized cabinet until use. The ϕX174 were propagated in the host *E. coli C* obtained from the *E. coli* Genetic Stock Center at Yale University (New Haven, CT) following the protocol developed previously.[11] *E. coli* were grown in LB media (35°C) in an exponential growth phase, corresponding to an optical density between 0.3 and 0.4. The ϕX174 was then added to the *E. coli* suspension and incubated at 35°C for 5 h with gentle shaking. The resulting suspension was centrifuged at 3500 rpm at 4°C at least three to four times to remove the lysate/debris. The supernatant containing the ϕX174 was decanted and stored at 4°C until use.

Zeta potential measurements

The membrane zeta potential was evaluated from the measured streaming potential as described elsewhere.[13] Potassium chloride (VWR, Randor, PA), sodium carbonate (EMD Millipore, Billerica, MA), sodium bicarbonate (EMD Millipore, Billerica, MA), acetic acid (EM Industries, Gibbstown, NJ), sodium acetate trihydrate (Sigma Aldrich, St. Louis, MO), citric acid monohydrate (Fisher Scientific, Fair Lawn, NJ), and disodium hydrogen phosphate (Amresco, Solon, OH) were used to prepare buffered salt solutions. The solution ionic strength was adjusted using KCl, with pH adjusted using HCl (EM Iindustries, Gibbstown, NJ) or KOH (EM Industries, Gibbstown, NJ) as needed. The solution conductivity was measured using a Thermo Orion Conductivity meter (Thermo Scientific, Waltham, MA). All buffers were prefiltered through Supor-200 membrane (pore size 0.2 μm) (Pall, Port Washington, NY) under vacuum to remove any large particles or undissolved solids immediately prior to use.

Ag/AgCl electrodes were prepared using Ag wires (1 mm dia). The wires were straightened, lightly sanded, placed in concentrated nitric acid for 10 s, and rinsed with DI water. The cleaned Ag wire and a reducing electrode (steel wire) were each placed in separate beakers containing 1 M KCl. A Kimwipe was used as a salt-bridge between the beakers. The two wires were then connected to a DC power source with the current maintained approximately at 20 mA for 20 min. A uniform Ag/AgCl coating was formed over the silver wire. The electrodes were stored in 0.5 M KCl solution when not in use.

The streaming potential device consisted of two Plexiglas chambers. A 25 mm membrane disk was placed between the chambers and secured with an O-ring. Ag/AgCl electrodes were inserted into the chambers with the tips about 1 mm away from the membrane. The chambers were carefully filled with buffer solution at the desired pH. The feed port of one chamber was connected to a pressurized feed reservoir filled with additional buffer solution with the exit port of the other chamber directed to waste. The electrodes were connected to a Keithley 2000 multimeter (Cleveland, OH) to measure the streaming potential (E_z) as a function of transmembrane pressure (ΔP) between 14 and 35 kPa (2–5 psig) using an Ashcroft digital pressure regulator. The apparent zeta potential, ζ_{app}, was calculated from the slope ($dE_z/d\Delta P$) using the Helmholtz–Smoluchowski equation:

$$\zeta_{app} = \frac{\mu \Lambda_0}{\varepsilon_0 \varepsilon_r} \left(\frac{dE_z}{d\Delta P} \right) \tag{1}$$

where μ and Λ_0 are the viscosity (kg m^{-1} s^{-1}) and conductivity (S m^{-1}) of the buffer solution, respectively, ε_0 is the permittivity (A^2 s^4/m^3. kg) of vacuum, and ε_r is the dielectric constant. The experiments were run in triplicate at each pH.

Fluorescent labeling

Fluorescent dyes Cy5 and SYBR Gold were purchased from Sigma-Aldrich and Life Technologies, respectively. Cy5 labeling of bacteriophage was done according to the protocol described previously.[11] The bacteriophage solution was first concentrated to 4×10^{10} pfu mL^{-1} by centrifugation at 3800 rpm using a spin-concentrator with an Ultracel 100 kDa membrane (EMD Millipore, Billerica, MA) and then buffer exchanged into 0.1 M $NaHCO_3$ (pH 8.5). Nearly 1 mL of the phage solution (pH 8.5) was added to one bottle of solid Cy5 (~0.2-0.3 mg), and allowed to react for 1 h, with 1 min of vortexing at every 10 min. The labeled phage were thoroughly washed with at least 100 diavolumes of 0.1 M $NaHCO_3$ buffer (around 15 wash cycles) using the spin-concentrator to remove any free (unreacted) dye.

The SYBR Gold labeling protocol was developed based on published literature for labeling bacteriophage iEPS5.[14] About 10 mL of a ϕX174 suspension with concentration of 10^{10} pfu mL^{-1} was buffer exchanged and concentrated to 1 mL (10^{11} pfu mL^{-1}) phage in 1X TAE buffer (MediaTech,

Manassas, VA) using a spin concentrator. 1 μL of SYBR Gold (10^4 X) dissolved in DMSO was added to the phage suspension. The solution was vortexed and allowed to react at room temperature for 20 min in the dark. Residual free dye was removed from the reaction mixture using 100 diavolumes of 1X TAE buffer. The labeled phage were stored at 4°C and diluted before use.

Virus filtration

Virus filtration experiments were conducted with single layers of the Viresolve® NFP membranes housed directly in a 47 mm diameter stainless steel filter holder (EMD Millipore Corp., Bedford, MA) without any additional support layer. These asymmetric membranes were used with the shiny side (i.e., skin-side) down as per the manufacturer's recommendation. This allows the more open support region to act as a "depth filter" protecting the skin layer from fouling.[15] Acetate (pH 4.9), PBS (pH 7.8), and carbonate (pH 10) buffers were prepared with DI water as per established procedures. Bacteriophage suspensions were added to the appropriate buffer, ultrasonicated for 45 min, and then prefiltered through a syringe filter housing a 0.2 μm cellulose acetate membrane immediately before being added to a 1-L feed reservoir, which was connected to the filter holder by plastic tubing. The reservoir was air-pressurized, with the pressure controlled at 210 kPa (30 psi) using an Ashcroft pressure regulator. Approximately 1 mL filtrate fractions were collected in centrifuge tubes. For the pressure release experiments, ~12 mL of unlabeled phage was challenged through the membrane, the pressure was released for about 10 min (no transmembrane pressure), and then the filtration was resumed for another 12 mL at 210 kPa.

pfu assay

Bacteriophage concentrations were determined using a plaque forming unit (pfu) assay.[11] Hard agar plates were prepared by pouring 10 g L^{-1} Difco Agar (BD-214530) in LB media after autoclaving the media for 40 min. Phage samples were appropriately diluted with DI water to obtain easily countable plaques (typically between 2 and 50 plaques/plate). Soft agar (4 g L^{-1} Difco Agar in LB media) was liquefied by heating in a microwave. 100 μL of the phage samples were then mixed with 200 μL of *E. coli* suspension and 900 μL of melted soft agar, and the resulting suspension was poured onto the hard agar plates. The plates were incubated for 8 h at 35°C before manually counting the number of plaques.

Confocal laser scanning microscopy

Confocal images were obtained after a virus filtration run with a pressure disruption. The membrane was first challenged with 12 mL of Cy5-labeled phage at 210 kPa; the pressure was released for ~10 min; the feed reservoir was emptied, washed, and refilled with a suspension containing the SYBR Gold labeled phage. The system was then repressurized to 210 kPa, and the filtration was continued for an additional 12 mL.

Virus filtration membranes were imaged with an Olympus Fluoview™ 1000 confocal laser scanning microscope (Olympus American Inc., New Jersey). Membranes were cut into small pieces (1.5 cm × 1 cm) and mounted on separate glass slides. The membranes were wet with a small drop of 10% glycerol, covered with a glass coverslip, and sealed using nail-polish. The membrane specimen was placed over a 100× oil objective lens (Numerical Aperture, NA = 1.25). The Cy5 and SYBR Gold dyes were excited with 488 nm (blue) and 610 nm (red) lasers, respectively, and imaged at emission wavelengths of 510 and 670 nm, with the zoom magnification of the lens set at 2.0. Optical cross-sectioning was done at 0.3-μm intervals, with images at multiple *x-y* planes stacked to reconstruct a z-image through the depth of the membrane using the Olympus Fluoview™ software. Viresolve® NFP membranes (thickness of 140 μm) were scanned from both sides (flipping the membrane in the microscope) since the maximum working distance of the oil objective lens is about 80 μm. The two acquired images were subsequently combined to generate a scan through the full depth of the membrane.

Results and Analysis

Typical data for retention of the bacteriophage ϕX174 by the Viresolve® NFP membrane during a constant pressure filtration experiment performed at a pressure of 210 kPa (30 psi) are shown in Figure 1. The results are plotted as the log reduction value:

$$\mathrm{LRV} = -\log_{10}\left(\frac{C_{\mathrm{filtrate}}}{C_{\mathrm{Feed}}}\right) \tag{2}$$

where the ϕX174 concentrations in the filtrate and feed solutions were determined by the plaque forming assay. The x-axis is the cumulative volumetric throughput, defined as the cumulative filtrate volume (V) divided by the membrane cross-sectional area (A). Data were obtained at a feed concentration of ~2×10^7 pfu mL^{-1} with the ϕX174 suspended in acetate (pH 4.9), phosphate (pH 7.8), and carbonate (pH 10) buffers, respectively. In each case, the buffer concentration was 1 mM with the total ionic strength adjusted using KCl to either 13 mM (left panel) or 40 mM (right panel). The use of low buffer concentrations (<10% of the total salt) minimized any effects associated with the specific buffer type used in each experiment. The small process volumes (<10 L m^{-2}) were used to minimize the volume of phage required in each experiment and to minimize artifacts associated with membrane fouling; the filtrate flux remained nearly constant throughout the constant pressure filtration, varying from ~7.7×10^{-5} m s^{-1} (280 L m^{-2} h^{-1}) at the start of the experiment to 6.4×10^{-5} m s^{-1} (240 L m^{-2} h^{-1}) after filtration of about 10 mL (~8 L m^{-2}). The flux was also independent of solution pH and ionic strength (variations of <±10%).

The virus retention was essentially constant throughout the virus filtration experiments. There was no evidence of any LRV decline, although this phenomenon might well occur at much larger throughput.[16] Data are not shown for V/A < 2 L m^{-2} since the measured phage concentrations under these conditions were reduced by dilution of the filtrate samples by the liquid hold-up volume from within the filter holder.[11] Note that the LRV seen in Figure 1 are significantly lower than those reported in the literature for the Viresolve® NFP filter since these experiments were performed with a single layer of membrane; the commercial NFP filters use 3 layers of the PVDF membrane in series providing approximately three times the LRV.[15] The LRV in the lower ionic strength

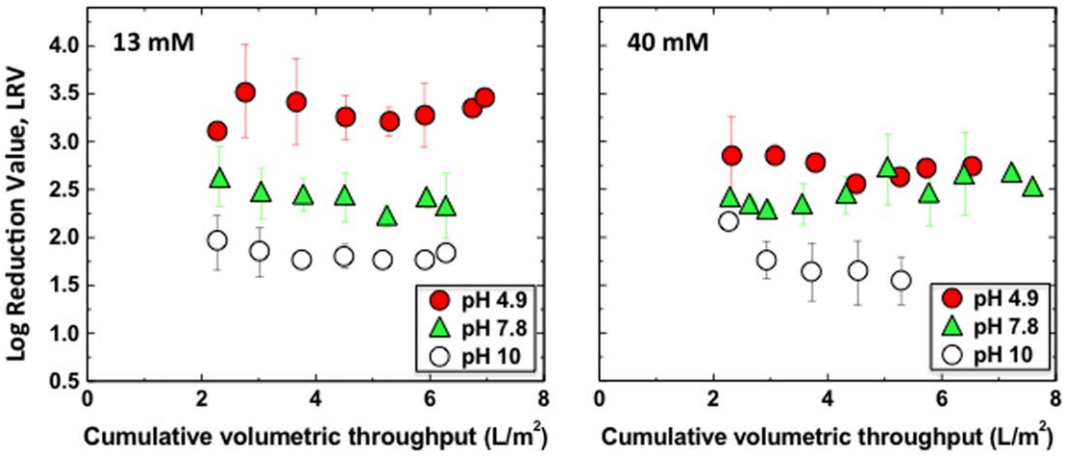

Figure 1. Log reduction values (LRV) during constant pressure filtration of the bacteriophage ϕX174 through Viresolve® NFP membranes at 210 kPa at pH 4.9, 7.8 and 10 at ionic strengths of 13 mM (left panel) and 40 mM (right panel).

solution (left panel) are a strong function of solution pH, with the greatest virus retention seen at pH 4.9 and the lowest seen at pH 10. The effect of solution pH was much less pronounced in the 40 mM ionic strength solution (right panel). The virus LRV at pH 4.9 decreased from 3.5 ± 0.3 in the low ionic strength solution to 2.8 ± 0.2 in the 40 mM solution, consistent with the greater shielding of electrostatic interactions in the higher ionic strength solution. In contrast, virus retention at pH 7.8 and pH 10 were nearly independent of the solution ionic strength (LRV = 2.5 ± 0.3 in both the 13 and 40 mM ionic strength solutions). LRV data at higher ionic strength (190 mM) showed an even weaker dependence on solution pH, with the LRV = 2.0 ± 0.5 for pH between 4.9 and 10 (data not shown).

To understand the effects of solution pH and ionic strength on the retention of the bacteriophage ϕX174, the zeta potential of the Viresolve® NFP membrane was determined from streaming potential measurements. The streaming potential data at each pH were highly linear, with r^2 values > 0.98, allowing the apparent zeta potential to be calculated directly from Eq. (1). Results are plotted in Figure 2 as a function of the solution pH; the error bars on the individual data points represent plus/minus one standard deviation for the three repeat measurements. The apparent zeta potential was negative at all measured pH values, with ζ_{app} going from -7.7 mV at pH 2.7 to -14 mV at pH 10. The surface charge of ϕX174 has been measured by chromatofocusing,[17] electrophoretic mobility,[18] and capillary isoelectric focusing,[19] with most values of the isoelectric point around pH 6.6.[20] Thus, the ϕX174 will be negatively-charged at pH 7.8 and 10, but will have a significant positive charge at pH 4.9. As a result, there should be an attractive electrostatic interaction between the ϕX174 and the Viresolve® NFP membrane at pH 4.9, which likely explains the increased retention seen in Figure 1 at this pH and low ionic strength.

Previous work by Dishari et al.[11] showed that a disruption in the filtration process (in this case a short period with no applied pressure) caused a significant increase in virus transmission through the Viresolve® NFP membrane at pH 10. A series of "pressure disruption" experiments were performed to evaluate the effects of solution pH and ionic strength on this phenomenon. In each case, the filtration was performed at a constant pressure of 210 kPa (30 psi) for a cumulative filtrate volume of $\sim$7 L m^{-2}. The transmembrane pressure

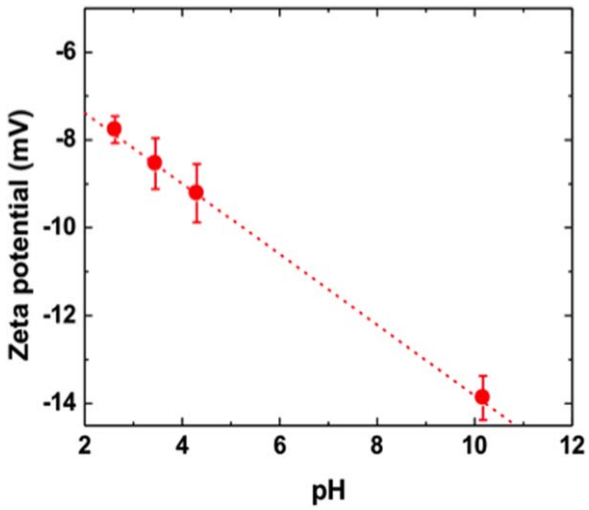

Figure 2. Zeta potential of Viresolve® NFP membrane as a function of pH.

Error bars represent plus/minus one standard deviation in repeat experiments.

was then released, with no filtration for a period of 10 min, after which the transmembrane pressure was reapplied and the filtration continued at 210 kPa for another 7 L m^{-2}. Filtrate samples were taken periodically to evaluate the LRV, with the results summarized in Figures 3 and 4 for high and low ionic strength (190 and 13 mM), respectively. In each case, the multiple symbols at the different pH represent data from replicate experiments performed using different membrane samples obtained from the same lot of membrane.

The LRV values in the high ionic strength solution were essentially independent of solution pH; repeat runs at all three pH values were nearly identical. In each case, the initial LRV was approximately 2.0 ± 0.4, with a slight decline over the first 6 L m^{-2} (although this was not statistically significant). The pressure release caused a sharp decline in LRV, with the LRV obtained immediately after the pressure release being close to zero (i.e., no virus retention). The LRV gradually increased over the 7 L m^{-2}, with the final LRV being very similar to that obtained before the pressure release. This recovery in LRV clearly indicates that the pressure disruption caused no irreversible damage to the membrane, consistent with results presented previously.[10,11]

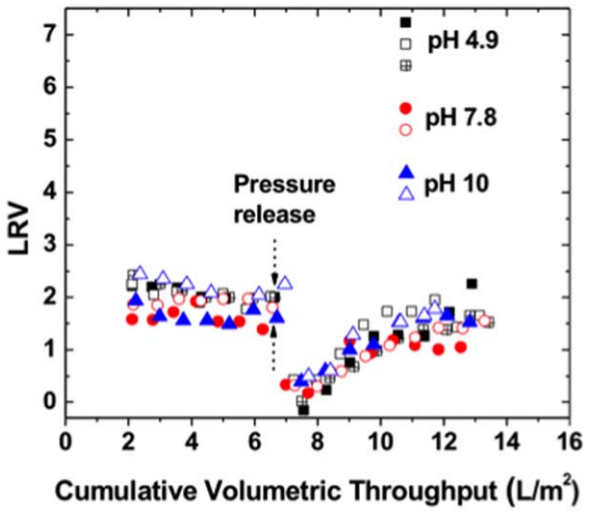

Figure 3. Log reduction values (LRV) during pressure disruption experiments using the Viresolve® NFP membranes at an ionic strength of 190 mM.

The dashed vertical line shows the point where the pressure was released. Multiple symbols at each pH represent data from replicate experiments.

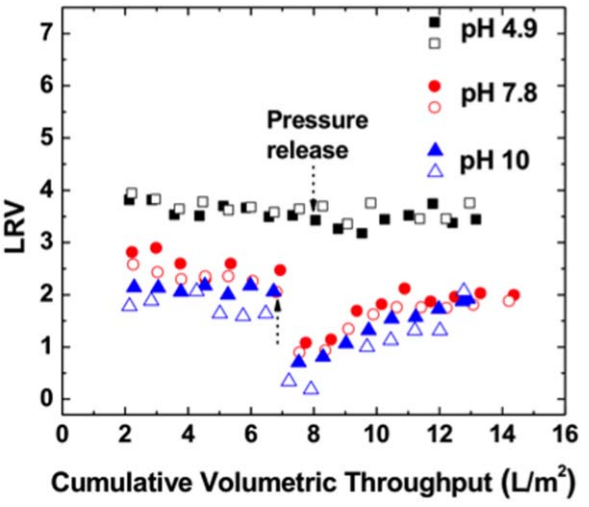

Figure 4. Log reduction values (LRV) during pressure disruption experiments using the Viresolve® NFP membranes at an ionic strength of 13 mM.

The dashed vertical lines show the points where the pressure was released. Multiple symbols at each pH represent data from replicate experiments.

Corresponding data at low ionic strength (13 mM) are shown in Figure 4. The results at pH 7.8 and 10 are similar to those seen in Figure 3, with the LRV values shifted up by about 0.5-log both before and after the pressure release. However, the situation is very different at pH 4.9. In this case, the pressure release caused no measurable change in the LRV; virus retention was essentially constant throughout the entire filtration experiment even with the pressure disruption at a cumulative filtrate volume of V/A = 6-8 L m^{-2}. These data suggest that the presence of electrostatic attractive interactions between the negatively charged membrane and the positively charged virus at low pH and low ionic strength eliminates the effects of a pressure disruption. This behavior is discussed in more detail subsequently.

Additional insights into the effects of solution conditions on virus retention during the pressure disruption experiments were obtained using confocal microscopy. The Viresolve® NFP membrane was first challenged with ~8 L m^{-2} of the Cy5-labeled (red) ϕX174 bacteriophage, the pressure was removed for ~10 min, and the membrane was then challenged with ~8 L m^{-2} of the SYBR Gold-labeled (green) phage. Figure 5 shows confocal images of the lower half (~80 μm) of the NFP membranes obtained after pressure release experiments performed at pH 4.9 (left panel) and pH 10 (right panel). The middle and bottom panels represent the single fluorescence channels showing emission at 510 and 670 nm, respectively, while the top panel provides an overlay of the two images. Note that the overlay is done automatically within the Olympus Fluoview™ software (without any manual alignment).

The images at both pH values show that the majority of the ϕX174 are captured in a diffuse band, having two distinct layers, located ~20 μm above the exit of the filter (120 μm into the filter depth if measured from the upstream surface of the filter). Similar results were seen in experiments performed without a pressure disruption as shown in Dishari et al.[11] Virus capture at this particular location may reflect the gradation in pore size within the Viresolve® NFP membrane. The thickness of this band is somewhat greater at pH 4.9, with a much higher relative contribution from the Cy5-labeled (red) phage. In addition, there is a very thin band right at the exit of the Viresolve® NFP membrane. However, this band is composed almost entirely of Cy5-labeled phage (present in the challenge before the pressure disruption) for the experiment performed at pH 10, while it is composed almost entirely of the SYBR Gold-labeled (green) phage (present in the challenge after the pressure disruption) at pH 4.9.

These differences in capture profiles are likely due the difference in electrostatic interactions at the high and low pH. At pH 10, some of the phage that were initially captured in the Viresolve® NFP filter are able to diffuse out of the pores when the pressure is released.[10,11] These (red) phage migrate deeper into filter and are either captured near the filter exit (narrow red band) or pass directly into the permeate (as seen by the very low LRV immediately after the pressure disruption in Figures 3 and 4). In contrast, the images in Figure 5 suggest that the red phage that were captured during the initial challenge remain trapped during the pressure release, most likely due to the attractive electrostatic interactions between the negatively-charged membrane and the positively charged phage under these conditions, thereby eliminating the increase in virus transmission when the pressure is reapplied (Figure 4). The green phage that are present in the challenge after the pressure release are simply captured in the diffuse band within the depth of the filter or in the fairly narrow band near the filter exit.

Discussion

The results presented in this study clearly demonstrate that virus retention by the Viresolve® NFP membrane is a function of solution pH and ionic strength. In particular, virus retention is increased by nearly 1-log by operating at low pH (4.9) and low ionic strength (13 mM), conditions that lead to significant attractive electrostatic interactions between the negatively-charged membrane and the positively charged ϕX174 (isoelectric point around pH 6.6). In addition, the use of low pH and low ionic strength eliminated the spike in virus transmission seen after a pressure disruption. These

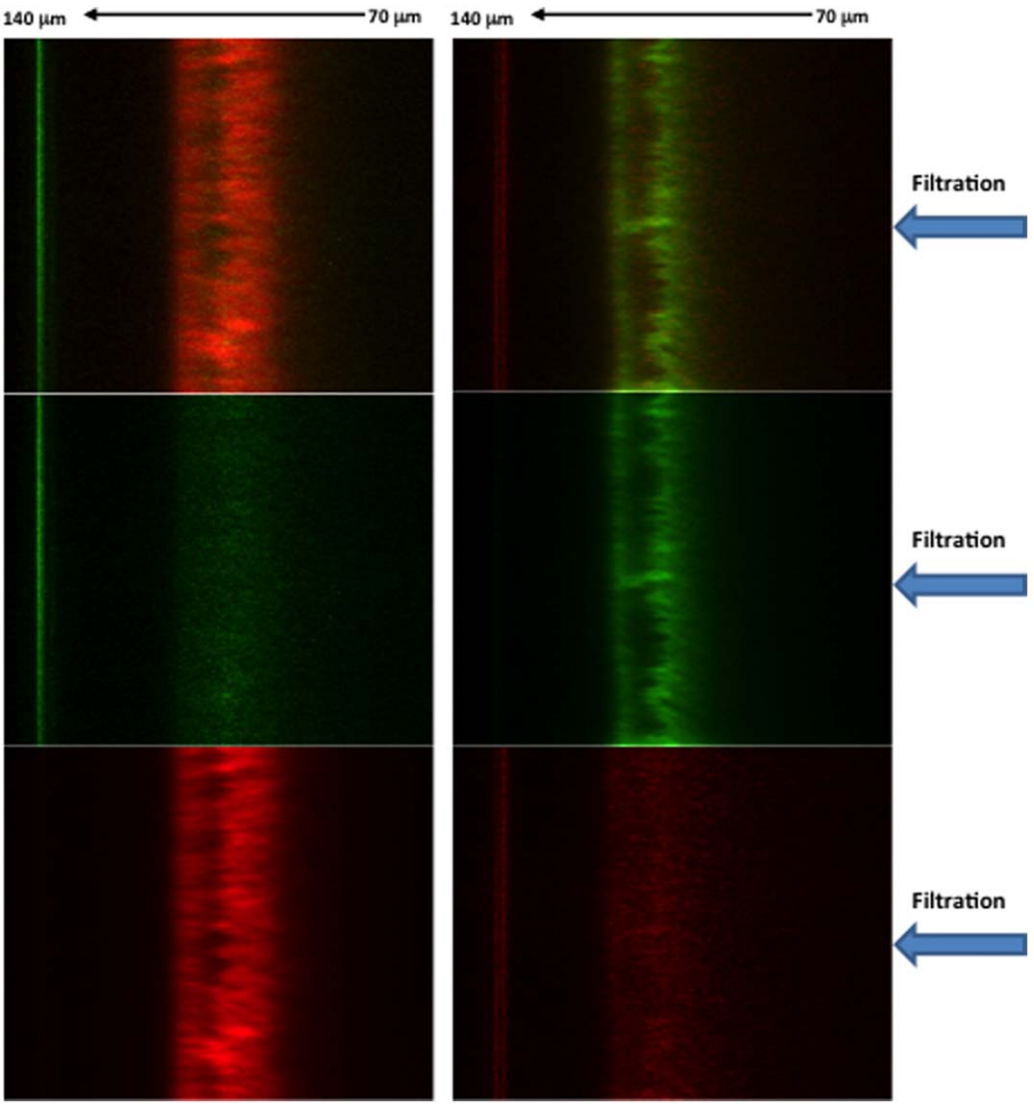

Figure 5. Confocal images of the lower half of the Viresolve® NFP membrane after a pressure release experiment. The membranes were challenged with Cy5-labeled (red) phage for 8 L m^{-2} followed by SYBR Gold-labeled (green) phage after the pressure release.

The left and right images correspond to experiments performed at pH 4.9 and 10, respectively, both with 13 mM ionic strength. The individual panels show results for: excitation of Cy5 (lower), excitation of SYBR Gold (middle), excitation of both dyes (upper).

are, to the best of our knowledge, the first published data quantifying the effect of solution conditions on virus retention in response to a process disruption similar to that which would occur when using multiple feed tanks, a final buffer flush to recover residual product from the virus filter, or in response to equipment error.

Woods and Zydney[10] and Dishari et al.[11] both attributed the increase in virus transmission after a process disruption to the diffusion of previously captured virus out of the pores, allowing them to migrate deeper into and possibly through the filter when the filtration is resumed. The data obtained at pH 4.9 and 13 mM ionic strength suggest that attractive electrostatic interactions can keep the virus "trapped" in the pore, even in the absence of any positive filtration, thereby eliminating the spike in virus transmission upon reapplication of the filtration pressure. This behavior was confirmed by confocal microscopy, with data at high pH showing migration of fluorescently labeled phage that were captured during the initial challenge deeper into the filter after the process disruption. This migration was not seen at low pH, with the previously captured phage remaining in the same location within the filter.

Virus filtration in downstream processing is typically done after the primary purification step, e.g., after a Protein A affinity column for initial capture/purification in the production of monoclonal antibody products. But, different manufacturers perform virus filtration at different places in the overall process relative to other (typically chromatography) processing steps. The data obtained in this study clearly demonstrate that the overall viral clearance and robustness of the virus filtration step can be significantly improved by performing the virus filtration at low pH, i.e., under conditions where there are attractive electrostatic interactions between typical viruses and the virus filtration membrane. It might also be possible to further enhance the virus removal capabilities, while minimizing adverse effects associated with process disruptions, by designing virus filters with surface charge characteristics that enhance the type of attractive interactions seen in this work at pH 4.9 with the ϕX174 bacteriophage and the Viresolve® NFP membrane. However,

this could create regulatory challenges since many downstream processes already use other methods (e.g., chromatographic adsorption) based on electrostatic interactions that would no longer be considered to function using an orthogonal clearance mechanism. Future studies will be needed to demonstrate the generality of this behavior with other virus filters and with viruses having different surface charge (and possibly hydrophobicity).

Acknowledgments

The authors acknowledge financial support from the Lilly Research Award Program (LRAP) from Eli Lilly and Company and from the NSF REU Program at The Pennsylvania State University. The authors also thank EMD Millipore for providing the single layer Viresolve® NFP membranes and Professor Wayne Curtis and his research group for assistance with bacteriophage propagation and the pfu assay.

Literature Cited

1. Miesegaes G, Lute S, Brorson K. Analysis of viral clearance unit operations for monoclonal antibodies. *Biotechnol Bioeng*. 2010;106:238–246.
2. Herath G, Yamamoto K, Urase T. Removal of viruses by microfiltration membranes at different solution environments. *Water Sci Technol*. 1999;40:331–338.
3. Oshima KH, Evans-Strickfaden TT, Highsmith AK, Ades EW. The use of a microporous polyvinylidene fluoride (PVDF) membrane filter to separate contaminating viral particles from biologically important proteins. *Biologicals*. 1996;24:137–145.
4. Pierre G, Furiga A, Berge M, Roques C, Aimar P, Causserand C. Protocol for the assessment of viral retention capability of membranes. *J Membr Sci*. 2011;381:41–49.
5. Yokoyama T, Murai K, Murozuka T, Wakisaka M, Tanifuji M, Fujii N, Tomono T. Removal of small non-enveloped viruses by nanofiltration. *Vox Sanguinis*. 2004;86:225–229.
6. Lukasik J, Scott TM, Andryshak D, Farrah SR. Influence of salts on virus adsorption to microporous filters. *Appl Environ Microbiol*. 2000;66:2914–2920.
7. Troccoli NM, McIver J, Losikoff A, Poiley J. Removal of viruses from human intravenous immune globulin by 35 nm nanofiltration. *Biologicals*. 1998;26:321–329.
8. Omar A, Kempf C. Removal of neutralized model parvoviruses and enteroviruses in human IgG solutions by nanofiltration. *Transfusion*. 2002;8:1005–1010.
9. Hirasaki T, Yokogi M, Kono A, Yamamoto N, Manabe SI. Removal and determination of dispersion state of bacteriophage Phi X174 in aqueous solution by cuprammonium regenerated cellulose microporous hollow fiber membrane (BMM). *J Membr Sci*. 2002;210:95–102.
10. Woods MA, Zydney AL. Effects of a pressure release on virus retention with the Ultipor DV20 membrane. *Biotechnol Bioeng*. 2014;111:545–551.
11. Dishari SK, Venkiteshwaran A, Zydney AL. Probing effects of pressure release on virus capture during virus filtration using confocal microscopy. *Biotechnol Bioeng*. 2015. doi: 10.1002/bit.25614
12. Jackson NB, Bakhshayeshi M, Zydney AL, Mehta A, van Reis R, Kuriyel R. Internal virus polarization model for virus retention by the Ultipor® VF grade DV20 membrane. *Biotechnol Prog*. 2014;30:856–863.
13. Burns DB, Zydney AL. Buffer effects on the zeta potential of ultrafiltration membranes. *J Membr Sci*. 2000;172:39–48.
14. Choi Y, Shin H, Lee J-H, Ryu S. Identification characterization of a novel flagelum-dependent salmonella-infecting bacteriophage, iEPS5. *Appl Environ Microbiol*. 2013;79:4829–4837.
15. Lute S, Bailey M, Combs J, Sukumar M, Brorson K. Phage passage after extended processing in small-virus-retentive filters. *Biotechnol Appl Biochem*. 2007;47:144–151.
16. Lutz H, Ireland T, Bolton G, Siwak M. Viral filtration of plasma-derived human IgG: a case study using Viresolve NFP. *Biopharm Int*. 2004;17:38–41.
17. Brorson K, Shen H, Lute S, Perez JS, Frey DD. Characterization and purification of bacteriophages using chromatofocusing. *J Chromatogr A*. 2008;1207:110–121.
18. Aronino R, Dlugy C, Arkhangelsky E, Shandalov S, Oron G, Brenner A, Gitis V. Removal of viruses from surface water and secondary effluents by sand filtration. *Water Res*. 2009;43:87–96.
19. Horka M, Kubıcek O, Ruzicka F, Hola V, Malinovska I, Slais K. Capillary isoelectric focusing of native and inactivated microorganisms. *J Chromatogr A*. 2007;1155:164–171.
20. Michen B, Graule T. Isoelectric point of viruses. *J Appl Microbiol*. 2010;109:388–397.
21. Stuckey J, Strauss D, Venkiteshwaran A, Gao J, Luo W, Quertinmont M, O'Donnell S, Chen D. A novel approach to achieving modular retrovirus clearance for a parvovirus filter. *Biotechnol Prog*. 2014;30:79–85.
22. Roush DJ, Myrold A, Burnham MS, And JV, Hughes JV. Limits in virus filtration capability? Impact of virus quality and spike level on virus removal with xenotropic murine leukemia virus. *Biotechnol Prog*. 2015;31:135–144.
23. Venkiteshwaran A, Fogle J, Patnaik P, Kowle R, Chen D. Mechanistic evaluation of virus clearance by depth filtration. *Biotechnol Prog*. 2015;31:431–437.

Manuscript received Apr. 28, 2015, and revision received June 3, 2015.